Lecture Notes of TICMI
Vol. 25, 2024, 85–102

On Fluids in Angular Pipes and Wedge-Shaped Canals

George Jaiani*

I. Vekua Institute of Applied Mathematics & Faculty of Exact and Natural Sciences of I. Javakhishvili Tbilisi State University
11 University St., 0186 Tbilisi, Georgia

Jeffery-Hamel flow is the flow between two planes that meet at an angle and was analyzed by Jeffery (1915) and Hamel (1917).

We consider the flow between two surfaces that meet at the edge of a dihedral (angle), whose sides are the tangent planes, inclined, in general, of the surfaces at the edge of the above dihedral.

In the zero approximation of hierarchical models for fluids the full accordance is shown of peculiarities of setting the Dirichlet and Keldysh type boundary conditions by motion of the fluids in pipes of angular cross-sections with the results of experiments carried out by J. Nikuradse in L. Prandtl's Laboratory at University of Göttingen.

Keywords: Engular pipes, Wedge-Shaped canals, Boundary conditions for viscous fluids, Hierarchical models, Experiments for fluids, Diriclet and Keldysh type boundary value problems.

AMS Subject Classification: 76D07, 76D17, 35J70, 35J75, 35L80, 35L81.

Introduction

Jeffery-Hamel flow is the flow between two planes that meet at an angle and was first analyzed by Jeffery (1915) [1] and Hamel (1917) [2]. It has subsequently been studied by von Kármán and Levi-Civita [3], Nikuradse Johann (Ivane) [4], [5], [6] (see below Section 8), Dean [7], Rosenhead [8], Landau and Lifshitz [9], Fraenkel [10].

We consider the flow between two surfaces that meet at the edge of a dihedral (angle), whose sides are the tangent planes inclined, in general, of the surfaces at the edge of the above dihedral.

In the zero approximation of hierarchical models for fluids we will show the full accordance of peculiarities of setting the Dirichlet and Keldysh type boundary conditions by motion of the fluids in pipes of angular cross-sections with the results of experiments carried out by J. Nikuradse (see [4]-[6], [11] and also [12]) in L. Prandtl's Laboratory at University of Göttingen.

In other words we will prove mathematically that usual (common) for viscous fluid boundary condition of sticking (i.e., equality of the wall and the fluid velocities) at a wall near the edge of the dihedral angle should be replaced by the

* Corresponding author. Email: george.jaiani@gmail.com

ISSN: 1512-0511 print

boundedness of the fluid velocity in a neighborhood of the edge of the above dihedral.

In Section 1 we give a brief exposition of the 3D prismatic shell-like domains angular (tapered, cusped), in general, (see [13], [14], [15], [16]) and discuss a geometry of their cross-sections which will serve as cross-sections of pipes and divergent or convergent canals.

In Section 2 we introduce mathematical moments of functions.

In Section 3 we briefly sketch 3D governing equations of the Newtonian viscous fluid.

In Section 4 we present the governing equations of the models of the first and, second type in the $N = 0$ approximation (see also [17]).

In Section 5 we rewrite the governing equations of Section 4 for the case $h = h_0 x_2^{\kappa}$, $h_0, \kappa = const > 0$.

In Section 6 we formulate Dirichlet and Keldysh type BVPs for an equation with type and order degeneracy and give criteria of their well-posedness as a theorem.

In Section 7 we investigate well-posedness of BVPs for the equations of Section 5.

In Section 8 we briefly describe two experiments of J. Nikuradse [5], [6], [11], [12], compare results of Section 7 and Section 8, and make conclusions.

1. Prismatic shell-like 3D domains

First a few words about prismatic shells (see also [13]-[16]).

Let us consider prismatic shells (see, Figures 1 and etc., and also [13]-[16]), occupying 3D domain Ω with the projection ω (on the plane $x_3 = 0$) and the face surfaces

$$x_3 = \overset{(+)}{h}(x_1, x_2) \in C^2(\omega) \;\text{ and }\; x_3 = \overset{(-)}{h}(x_1, x_2) \in C^2(\omega), \;\; (x_1, x_2) \in \omega.$$

$$2h(x_1, x_2) := \overset{(+)}{h}(x_1, x_2) - \overset{(-)}{h}(x_1, x_2) > 0, \;\; (x_1, x_2) \in \omega, \tag{1}$$

is the thickness of the prismatic shell. A part of $\partial\omega$, where the thickness vanishes, i.e., $2h = 0$, is said to be a cusped edge. If in the symmetric case (see below Figure 3) $\partial\omega$ contains it smoothly, we shall call it a blunt edge, otherwise, i.e., the points of the cusped edge are points of nonsmoothness of $\partial\omega$, we shall call it a sharp edge (see Figures 2, 3). In the nonsymmetric case the cusp edge we shall call blunt provided at least one tangent to a profile is orthogonal to the shell projection (see Figures 6-12).

Let

$$2\tilde{h}(x_1, x_2) := \overset{(+)}{h}(x_1, x_2) + \overset{(-)}{h}(x_1, x_2), \;\; (x_1, x_2) \in \omega. \tag{2}$$

In the case of the symmetric prismatic shell, i.e., when

$$\overset{(-)}{h}(x_1, x_2) = -\overset{(+)}{h}(x_1, x_2),$$

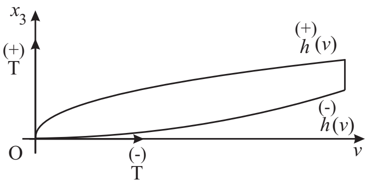

Figure 1. A prismatic shell of constant thickness. $\partial\Omega$ is a Lipschitz boundary

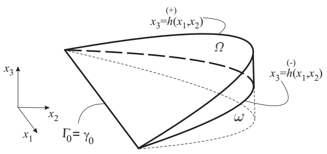

Figure 2. A sharp cusped prismatic shell with a semicircle projection. $\partial\Omega$ is a Lipschitz boundary

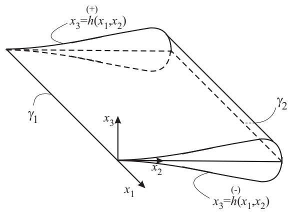

Figure 3. A cusped plate with sharp γ_1 and blunt γ_2 edges, $\gamma^0 := \gamma_1 \cup \gamma_2$. $\partial\Omega$ is a non-Lipschitz boundary

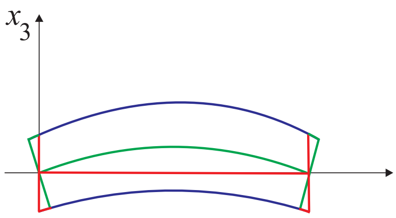

Figure 4. Comparison of cross-sections of prismatic and standard shells

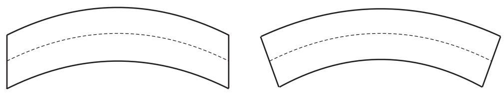

Figure 5. Cross-sections of a prismatic (left) and a standard shell with the same mid-surface

evidently

evidently

$$2\tilde{h}(x_1, x_2) \equiv 0, \quad (x_1, x_2) \in \omega.$$

Distinctions between the prismatic shell of a constant thickness and the standard shell of a constant thickness are shown in the Figures 4, 5, where cross-sections of the prismatic shell of a constant thickness with its projection and of the standard shell of a constant thickness with its middle surface are given in red and green colors, respectively, with common parts in blue. In other words, the lateral boundary of the standard shell is orthogonal to the "middle surface" of the shell, while the lateral boundary of the prismatic shell is orthogonal to the prismatic shell's projection on $x_3 = 0$ (see [15], [16])

In particular, let ω be a domain bounded by a sufficiently smooth arc $(\partial\omega \setminus \overline{\gamma^0})$ lying in the half -plane $x_2 > 0$ and a segment $\overline{\gamma^0}$ of the x_1-axis $(x_2 = 0)$. Let the thickness look like (see Figures 2, 3)

$$2h(x_1, x_2) = 2h_0 x_2^{\kappa}, \qquad h_0,\ \kappa = const > 0, \tag{3}$$

which corresponds to the case

$$\overset{(\pm)}{h}(x_1,x_2) = \overset{(\pm)}{h}_0 x_2^{\kappa}, \quad \overset{(\pm)}{h}_0 = const, \quad \overset{(+)}{h}_0 > \overset{(-)}{h}_0, \quad 2h_0 := \overset{(+)}{h}_0 - \overset{(-)}{h}_0.$$

In this case we have to do with a blunt edge for $\kappa < 1$ and with a sharp edge for $\kappa \geq 1$, respectively.

In Figures 6-20 ($\hat{\varphi}$ is the angle at the cusp between tangents $\overset{(+)}{T}$ and $\overset{(-)}{T}$, ν is an inward normal at O to $\partial\omega$) we show some characteristic (typical) profiles (cross-sections) of cusped prismatic shells.

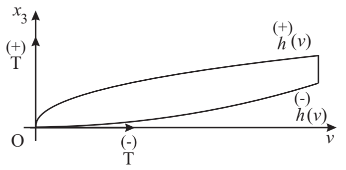

Figure 6. A cross-section of a blunt cusped prismatic shell ($\hat{\varphi} = \frac{\pi}{2}$). It has a Lipschitz boundary

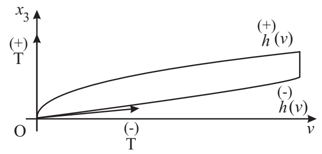

Figure 7. A cross-section of a blunt cusped prismatic shell ($\hat{\varphi} \in]0, \frac{\pi}{2}[$). It has a Lipschitz boundary

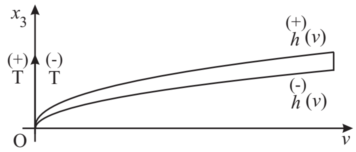

Figure 8. A cross-section of a blunt cusped prismatic shell ($\hat{\varphi} = 0$). It has a non-Lipschitz boundary

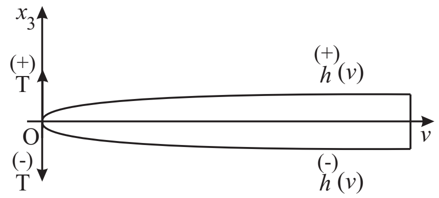

Figure 9. A cross-section of a blunt cusped plate ($\hat{\varphi} = \pi$). It has a Lipschitz boundary

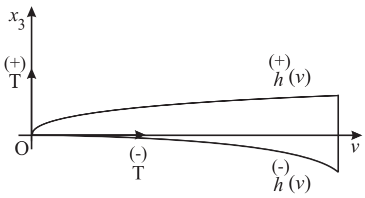

Figure 10. A cross-section of a blunt cusped prismatic shell ($\hat{\varphi} = \frac{\pi}{2}$). It has a Lipschitz boundary

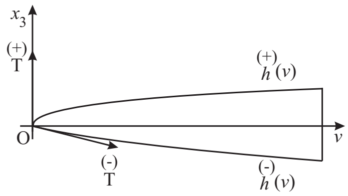

Figure 11. A cross-section of a blunt cusped prismatic shell ($\hat{\varphi} \in]\frac{\pi}{2}, \pi[$). It has a Lipschitz boundary

2. Mathematical moments of functions

The rth order moment of the function $f(x_1, x_2, x_3)$ is defined as follows (see [13]-[15], [18]):

$$f_r(x_1,x_2) := \int\limits_{\overset{(-)}{h}(x_1,x_2)}^{\overset{(+)}{h}(x_1,x_2)} f(x_1,x_2,x_3) P_r(ax_3 - b)dx_3, \quad r = 0,1,2,..., \tag{4}$$

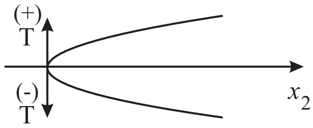

Figure 12. $\hat{\varphi} = \pi$

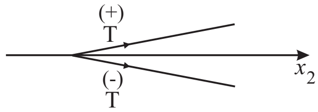

Figure 13. Wedge, $\hat{\varphi} \in]0, \pi[$

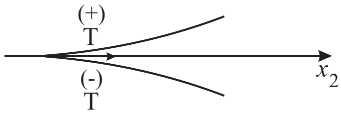

Figure 14. $\hat{\varphi} = 0$

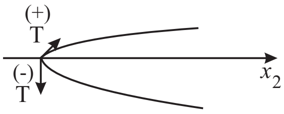

Figure 15. $\frac{\pi}{2} < \hat{\varphi} < \pi$

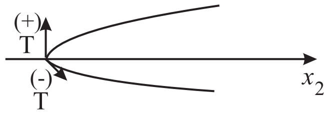

Figure 16. $\frac{\pi}{2} < \hat{\varphi} < \pi$

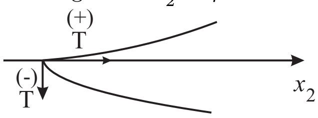

Figure 17. $\hat{\varphi} = \frac{\pi}{2}$

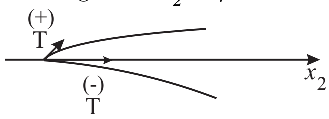

Figure 18. $0 < \hat{\varphi} < \frac{\pi}{2}$

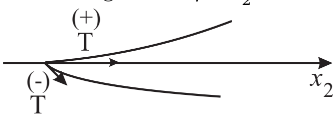

Figure 19. $0 < \hat{\varphi} < \frac{\pi}{2}$

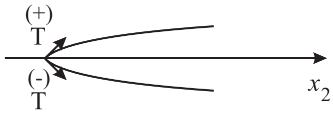

Figure 20. $0 < \hat{\varphi} < \pi$

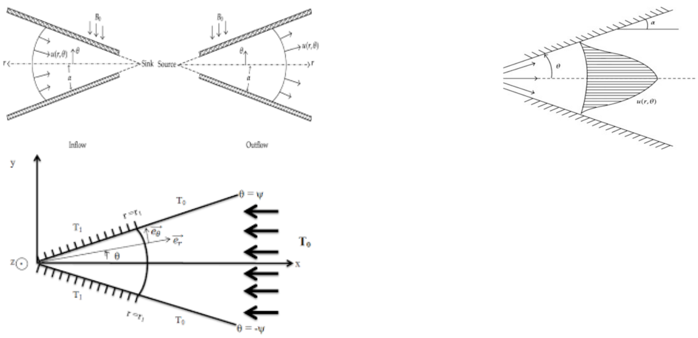

Figure 21. Divergent and convergent canals

where P_r Legandre Polynomials (see below (8)),

$$a(x_1, x_2) := \frac{1}{h(x_1, x_2)}, \quad b(x_1, x_2) := \frac{\widetilde{h}(x_1, x_2)}{h(x_1, x_2)}, \tag{5}$$

we remined

$$2h(x_1, x_2) = \overset{(+)}{h}(x_1,\, x_2) - \overset{(-)}{h}(x_1,\, x_2) > 0, \tag{6}$$

$$2\widetilde{h}(x_1, x_2) = \overset{(+)}{h}(x_1,\, x_2) + \overset{(-)}{h}(x_1,\, x_2) > 0, \tag{7}$$

$$P_r(\tau) = \frac{1}{2^r r!}\frac{d^r(\tau^2-1)^r}{d\tau^r}, \quad r = 0, 1, \cdots , \tag{8}$$

$$\tau = ax_3 - b = \frac{2}{\overset{(+)}{h}(x_1, x_2) - \overset{(-)}{h}(x_1, x_2)}x_3$$
$$-\frac{\overset{(+)}{h}(x_1, x_2) + \overset{(-)}{h}(x_1, x_2)}{\overset{(+)}{h}(x_1, x_2) - \overset{(-)}{h}(x_1, x_2)}, \tag{9}$$

$$\left(m + \frac{1}{2}\right)a \int\limits_{\overset{(-)}{h}(x_1,x_2)}^{\overset{(+)}{h}(x_1,x_2)} P_m(ax_3 - b)P_n(ax_3 - b)dx_3 = \delta_{mn}.$$

Sufficiently smooth function f may be represented as the following Fourier-Legendre series (see e.g. [13])

$$f(x_1, x_2, x_3) = \sum_{r=0}^{\infty} a\left(r + \frac{1}{2}\right)f_r P_r(ax_3 - b). \tag{10}$$

3. 3D governing equations of the Newtonian viscous fluid

Let us recall the governing equations of the Newtonian viscous fluid (see e.g., [19], Ch. 2 Conservation of mass and Momentum, Ch. 6 Viscosity and the Navier-Stokes equations and [20], Ch 1, §1 Classical fluids and Navier-Stokes system or [17]):

As is well known, motion of the Newtonian fluid is characterized by the following equations

$$\rho\frac{dv_i(x_1, x_2, x_3, t)}{dt} = \sigma_{ji,j}(x_1, x_2, x_3, t) + \Phi_i(x_1, x_2, x_3, t), \quad i = \overline{1, 3}, \tag{11}$$

$$\sigma_{ji} = -\delta_{ji}p + \lambda\delta_{ji}\vartheta(v) + 2\mu\epsilon_{ji}(v), \quad i, j = \overline{1, 3}, \tag{12}$$

$$\epsilon_{ji}(v) := \frac{1}{2}\left(v_{j,i+v_{i,j}}\right), \quad i, j = \overline{1, 3}, \tag{13}$$

$$\vartheta := \epsilon_{ii} = v_{k,k} =: \mathrm{div}v, \tag{14}$$

$$\lambda := \mu' - \frac{2}{3}\mu$$

where $v := (v_1, v_2, v_3)$ is a velocity vector, σ_{ij} is a stress tensor, ϵ_{ij} is a velocity tensor, p is a pressure, Φ_i, $i = \overline{1, 3}$, are components of the volume force, μ is the viscosity, μ' is the second viscosity[1], ρ is a density of the fluid. Throughout

[1] $\mu' = 0$ for the Stokes case, in gases μ' may be positive [19]

the paper we use, on the one hand Einstein's summation convention on repeated indices. Latin indices run values 1,2,3, while Greek indices run values 1,2 and on the other hand, the simplified notation for the partial derivative e.g.,

$$\frac{\partial \sigma_{ji}}{\partial x_j} =: \sigma_{ji,j}. \tag{15}$$

As well-known an incompressible fluid is defined as the fluid whose volume or density doesn't change with pressure (see e.g. [19], p. 6 and p. 17). In reality, rigorous incompressible fluid doesn't exist.

In the case of incompressible barotropic fluids, to the system (11)-(13) we add the equation

$$\mathrm{div} v = 0, \tag{16}$$

which expresses a fact that the velocity of change of cubical dilatation of each parcel of moving fluid is unchangeable (constant) during moving.

In general, for compressible fluids continuity equation has the form

$$\frac{d\rho}{dt} + \rho \mathrm{div} v = 0 \tag{17}$$

[this last equation can also be written as

$$\frac{\partial \rho}{\partial t} + \mathrm{div}(\rho v) = 0 \tag{18}$$

clearly, for $\rho = const$ from (17) we get again (16) and should be also added the state equation

$$\chi(\rho, p) = 0, \tag{19}$$

where χ is a certain function defining the state equation.

4. 2*D* governing equations of the models of the first and second type in the *N* = 0 approximation

Considering the governing equations (11)-(14) and (16) in the prismatic shell-like 3D domain containing the fluid under consideration and integrating within the limits $\overset{(-)}{h}(x_1, x_2)$ and $\overset{(+)}{h}(x_1, x_2)$ with respect to the thickness variable x_3, we obtain

$$\sigma_{\alpha\beta 0,\alpha} + \overset{0}{X}_\beta = \rho \frac{dv_{\beta 0}}{dt}, \quad i = \beta = 1, 2 \tag{20}$$

$$\sigma_{\alpha 30,\alpha} + \overset{0}{X}_3 = \rho \frac{dv_{30}}{dt}, \quad i = 3 \tag{21}$$

where

$$\overset{0}{X}_i := \overset{(+)}{\sigma}_{3i} - \overset{(+)}{\sigma}_{\gamma i} \overset{(+)}{h}_{,\gamma} - \overset{(-)}{\sigma}_{3i} + \overset{(-)}{\sigma}_{\gamma i} \overset{(-)}{h}_{,\gamma} + \Phi_{i0}, \quad i = \overline{1,3}$$

Providing as known stresses on the face surfaces, and, bearing in mind

$$v_k(x_1, x_2, x_3, t) = \frac{1}{2h(x_1, x_2, t)} v_{k0}(x_1, x_2, t),$$

from (12) we have correspondingly for $j = \beta$ and $j = 3$

$$\begin{aligned} &\sigma_{\alpha\beta 0} = -\delta_{\alpha\beta} p_0 + \lambda \delta_{\alpha\beta} \left(v_{\gamma 0,\gamma} - \tfrac{h_{,\gamma}}{h} v_{\gamma 0} \right) \\ &+\mu \left[\left(-\tfrac{h_{,\alpha}}{h} v_{\beta 0} - \tfrac{h_{,\beta}}{h} v_{\alpha 0} \right) + v_{\beta 0,\alpha} + v_{\alpha 0,\beta} \right] \\ &= -\delta_{\alpha\beta} p_0 + \lambda \delta_{\alpha\beta} h \widetilde{v}_{\gamma 0,\gamma} + \mu h \left(\widetilde{v}_{\alpha 0,\beta} + \widetilde{v}_{\beta 0,\alpha} \right), \quad \alpha, \beta = 1, 2, \end{aligned} \tag{22}$$

and

$$\sigma_{3\beta 0} = \mu \left(-\frac{h_{,\beta}}{h} v_{30} + v_{30,\beta} \right) = \mu h \widetilde{v}_{30,\beta}, \quad \beta = 1, 2; \tag{23}$$

$$\sigma_{330} = -p_0 + \lambda v_{\gamma 0,\gamma} \tag{24}$$

where

$$\widetilde{v}_{j0} := \frac{v_{j0}}{h}. \tag{25}$$

From (20) and (21) after substituting there (22) and (23) respectively, we obtain the following governing equations

$$(h\overset{0}{\widetilde{p}_0})_{,\beta} + \left[\lambda h \overset{0}{\widetilde{v}}_{\gamma 0,\gamma} \right]_{,\beta} + \left[\mu h \left(\overset{0}{\widetilde{v}}_{\alpha 0,\beta} + \overset{0}{\widetilde{v}}_{\beta 0,\alpha} \right) \right]_{,\alpha} + \overset{0}{X}_\beta = \rho h \frac{\partial \overset{0}{\widetilde{v}}_{\beta 0}}{\partial t}, \quad \beta = 1, 2;^{1} \tag{26}$$

$$\left(\mu h \overset{0}{\widetilde{v}}_{30,\alpha} \right)_{,\alpha} + \overset{0}{X}_3 = \rho h \frac{\partial \overset{0}{\widetilde{v}}_{30}}{\partial t}, \tag{27}$$

provided $\rho = \rho(x_1, x_2)$ and we consider Stoke's approximation.

[1] In terms of $\overset{0}{p}_0$ moment for presure the first term in (26), (30) looks like

$$\overset{0}{p}_{0,\beta},$$

because of

$$\overset{0}{\widetilde{p}_0} := \frac{\overset{0}{p}_0}{h}.$$

From (16) by virtue of (14), using integration by parts, we get to the system (26), (27) the additional equation

$$v_{\gamma 0,\gamma} - \frac{h_{,\gamma}}{h} v_{\gamma 0} = 0, \tag{28}$$

i.e., in terms of weighted moments (see (25))

$$(h\overset{0}{\widetilde{v}}_{\gamma 0})_{,\gamma} - h_{,\gamma}\overset{0}{\widetilde{v}}_{\gamma 0} = 0,$$

whence

$$\overset{0}{\widetilde{v}}_{\gamma 0,\gamma} = 0. \tag{29}$$

In the stationary case, bearing in mind (29), from (26) we obtain

$$(h\overset{0}{\widetilde{p}}_0)_{,\beta} + (\mu h)_{,\alpha}(\overset{0}{\widetilde{v}}_{\alpha 0,\beta} + \overset{0}{\widetilde{v}}_{\beta 0,\alpha}) + \mu h \overset{0}{\widetilde{v}}_{\beta 0,\alpha\alpha} + \overset{0}{X}_\beta = 0, \quad \beta = 1, 2.$$

Differentiating the last with respect to x_β and then summing over β we get

$$(h\overset{0}{\widetilde{p}}_0)_{,\beta\beta} + (\mu h)_{,\alpha\beta}(\overset{0}{\widetilde{v}}_{\alpha 0,\beta} + \overset{0}{\widetilde{v}}_{\beta 0,\alpha}) + (\mu h)_{,\alpha}\overset{0}{\widetilde{v}}_{\alpha 0,\beta\beta} + (\mu h)_{,\beta}\overset{0}{\widetilde{v}}_{\beta 0,\alpha\alpha} + \overset{0}{X}_{\beta,\beta} = 0,$$

So, having found $\overset{0}{\widetilde{v}}_{10}$, $\overset{0}{\widetilde{v}}_{20}$, from (26), we have got Poisson equation for p_0 and singular Poisson equation for $\overset{0}{\widetilde{p}}$.

4.1. *The first type model*

In the case of the first type model on the face surfaces stress vectors are assumed to be prescribed, while the values of velocities on the face surfaces are replaced by the first terms of their Fourier-Legendre expansions (see (10)):

$$\overset{(\pm)}{v}_i(x_1, x_2, x_3, t) := v_i(x_1, x_2, \overset{(\pm)}{h}(x_1, x_2), t) = \frac{1}{2h} v_{i0}(x_1, x_2, t).$$

The governing system as it follows correspondingly from (26) and (27), respectively, looks like:

$$(h\overset{0}{\widetilde{p}}_0)_{,\beta} + \Big[\lambda h \overset{0}{\widetilde{v}}_{\gamma 0,\gamma}\Big]_{,\beta} + \Big[\mu h\Big(\overset{0}{\widetilde{v}}_{\alpha 0,\beta} + \overset{0}{\widetilde{v}}_{\beta 0,\alpha}\Big)\Big]_{,\alpha} + \overset{0}{X}_\beta = \rho h \frac{\partial \overset{0}{\widetilde{v}}_{\beta 0}}{\partial t}, \tag{30}$$

$$\Big(\mu h \overset{0}{\widetilde{v}}_{30,\alpha}\Big)_{,\alpha} + \overset{0}{X}_3 = \rho h \frac{\partial \overset{0}{\widetilde{v}}_{30}}{\partial t}, \tag{31}$$

provided $\rho = \rho(x_1, x_2)$, we consider Stoke's approximation, and $\beta = 1, 2$.

From (16) we get the additional equation to system (30), (31)

$$v_{\gamma 0,\gamma} - \frac{h_{,\gamma}}{h} v_{\gamma 0} = 0, \tag{32}$$

i.e., in terms of weighted moments

$$(h\overset{0}{\widetilde{v}}_{\gamma 0})_{,\gamma} - h_{,\gamma}\overset{0}{\widetilde{v}}_{\gamma 0} = 0, \tag{33}$$

whence

$$\overset{0}{\widetilde{v}}_{\gamma 0,\gamma} = 0. \tag{34}$$

In the stationary case, bearing in mind (34), from (30) we obtain

$$(h\overset{0}{\widetilde{p}}_0)_{,\beta} + (\mu h)_{,\alpha}(\overset{0}{\widetilde{v}}_{\alpha 0,\beta} + \overset{0}{\widetilde{v}}_{\beta 0,\alpha}) + \mu h\overset{0}{\widetilde{v}}_{\beta 0,\alpha\alpha} + \overset{0}{X}_\beta = 0, \quad \beta = 1,2. \tag{35}$$

Differentiating the last with respect to x_β and then summing with respect to β we get

$$\begin{aligned}(h\overset{0}{\widetilde{p}}_0)_{,\beta\beta} + (\mu h)_{,\alpha\beta}(\overset{0}{\widetilde{v}}_{\alpha 0,\beta} + \overset{0}{\widetilde{v}}_{\beta 0,\alpha}) + (\mu h)_{,\alpha}\overset{0}{\widetilde{v}}_{\alpha 0,\beta\beta} \\ + (\mu h)_{,\beta}\overset{0}{\widetilde{v}}_{\beta 0,\alpha\alpha} + \overset{0}{X}_{\beta,\beta} = 0.\end{aligned} \tag{36}$$

Therefore, if $\mu h = const$ we have

$$(h\overset{0}{\widetilde{p}}_0)_{,\beta\beta} = -\overset{0}{X}_{\beta,\beta}. \tag{37}$$

Further, in the stationary case from (35) and (31) it follows

$$\overset{0}{\widetilde{v}}_{\beta 0,\alpha\alpha} = -\frac{1}{\mu h}\Big[\overset{0}{X}_\beta + (h\overset{0}{\widetilde{p}}_0)_{,\beta}\Big], \quad \beta = 1,2, \tag{38}$$

and

$$\Big(\mu h\overset{0}{\widetilde{v}}_{30,\alpha}\Big)_{,\alpha} = -\overset{0}{X}_3. \tag{39}$$

Remark 5. If $h =$ const by virtue of (34), clearly, (30) takes the form

$$\overset{0}{\widetilde{p}}_{0,\beta} + \mu\overset{0}{\widetilde{v}}_{\beta 0,\alpha\alpha} + h^{-1}\overset{0}{X}_\beta = \rho\frac{\partial\overset{0}{\widetilde{v}}_{\beta 0}}{\partial t}, \quad \beta = 1,2, \tag{40}$$

differentiating the last with respect to x_β and then summing over β we obtain

$$\overset{0}{\widetilde{p}}_{0,\beta\beta} + h^{-1}\overset{0}{X}_{\beta,\beta} = \Big[\rho\frac{\partial\overset{0}{\widetilde{v}}_{\beta 0}}{\partial t}\Big]_{,\beta} = \rho_{,\beta}\frac{\partial\overset{0}{\widetilde{v}}_{\beta 0}}{\partial t}. \tag{41}$$

4.2. *The second type model*

Now, we construct the second type of hierarchical models for Newtonian viscous fluids, acting similarly as at the beginning of Section 4 but this time we assume that on the face surfaces the velocities are prescribed and by calculations during constructing the hierarchical models values of the stress vector components on the face surfaces are replaced by the first term

$$\overset{(\pm)}{\sigma}_{ji}(x_1, x_2, x_3) = \frac{1}{2h}\sigma_{ji0}(x_1, x_2) = \frac{1}{2}\widetilde{\sigma}_{ji0}(x_1, x_2), \quad i, j = \overline{1, 3}. \tag{42}$$

of their Fourier-Legendre expansions:

$$\sigma_{ji} = \sum_{r=0}^{\infty} a\left(r + \frac{1}{2}\right)\sigma_{jir}P_r(ax_3 - b), \quad i, j = \overline{1, 3}, \tag{43}$$

we arrive at the governing system of the following form (see [17], and also [22])

$$\begin{aligned}
&-q_{0,\beta} + \left\{\lambda\left[(\ln h)_{,\gamma}\overset{0}{\widetilde{v}}_{\gamma 0} + \frac{1}{2}\overset{0}{\Psi}_{l'l'}\right]\right\}_{,\beta} + \left\{\mu\left[(\overset{0}{\widetilde{v}}_{\alpha 0,\beta} + \overset{0}{\widetilde{v}}_{\beta 0,\alpha}) + (\ln h)_{,\beta}\overset{0}{\widetilde{v}}_{\alpha 0}\right.\right.\\
&\quad \left.\left. + (\ln h)_{,\alpha}\overset{0}{w}_{\beta 0} + h^{-1}\overset{0}{\Psi}_{\alpha\beta}\right]\right\}_{,\alpha} + \overset{0}{Y}_{\beta} = \rho h^{-1}\frac{\partial v_{\beta 0}}{\partial t} = \rho\frac{\partial \widetilde{v}_{\beta 0}}{\partial t}, \quad \beta = 1, 2,
\end{aligned} \tag{44}$$

$$\left\{\mu\left[\overset{0}{\widetilde{v}}_{30,\alpha} + (\ln h)_{,\alpha}\overset{0}{\widetilde{v}}_{30}\right]\right\}_{,\alpha} + h^{-1}\overset{0}{\Psi}_{\alpha 3,\alpha} + \overset{0}{Y}_3 = \rho h^{-1}\frac{\partial v_{30}}{\partial t} = \rho\frac{\partial \widetilde{v}_{30}}{\partial t}, \tag{45}$$

where $\overset{0}{Y}_j = \frac{1}{h}\Phi_{j0}$, $j = \overline{1, 3}$, $\overset{0}{\Psi}_{ji}$ depend linearly on the values of the velocities on the face surfaces, namely,

$$\begin{aligned}
\overset{0}{\Psi}_{\alpha\beta} :=& -\widetilde{v}_\alpha(x_1, x_2, \overset{(+)}{h}(x_1, x_2), t)\overset{(+)}{h}_{,\beta} + \widetilde{v}_\alpha(x_1, x_2, \overset{(-)}{h}(x_1, x_2), t)\overset{(-)}{h}_{,\beta}\\
& -\widetilde{v}_\beta(x_1, x_2, \overset{(+)}{h}(x_1, x_2), t)\overset{(+)}{h}_{,\alpha} + \widetilde{v}_\beta(x_1, x_2, \overset{(+)}{h}(x_1, x_2), t)\overset{(+)}{h}_{,\alpha};
\end{aligned}$$

$$\begin{aligned}
\overset{0}{\Psi}_{\alpha 3} :=& \ \widetilde{v}_\alpha(x_1, x_2, \overset{(+)}{h}(x_1, x_2), t) - \widetilde{v}_\alpha(x_1, x_2, \overset{(-)}{h}(x_1, x_2), t)\\
& -\widetilde{v}_3(x_1, x_2, \overset{(+)}{h}(x_1, x_2), t)\overset{(+)}{h}_{,\alpha} + \widetilde{v}_3(x_1, x_2, \overset{(+)}{h}(x_1, x_2), t)\overset{(+)}{h}_{,\alpha};
\end{aligned}$$

$$\begin{aligned}
\overset{0}{\Psi}_{3\beta} :=& -\widetilde{v}_3(x_1, x_2, \overset{(+)}{h}(x_1, x_2), t)\overset{(+)}{h}_{,\beta} + \widetilde{v}_\alpha(x_1, x_2, \overset{(-)}{h}(x_1, x_2), t)\overset{(+)}{h}_{,\beta}\\
& +\widetilde{v}_\beta(x_1, x_2, \overset{(+)}{h}(x_1, x_2), t) - \widetilde{v}_\beta(x_1, x_2, \overset{(+)}{h}(x_1, x_2), t);
\end{aligned}$$

$$\overset{0}{\Psi}_{\alpha 3} := \widetilde{v}_3(x_1, x_2, \overset{(+)}{h}(x_1, x_2), t) - \widetilde{v}_3(x_1, x_2, \overset{(-)}{h}(x_1, x_2), t).$$

$$(h\overset{0}{\widetilde{v}}_{\gamma 0})_{,\gamma} + \overset{0}{V} = 0 \tag{46}$$

with

$$\begin{aligned}\overset{0}{V} := & -\widetilde{v}_\alpha(x_1, x_2, \overset{(+)}{h}(x_1,x_2),t)\overset{(+)}{h}_{,\alpha} + \widetilde{v}_\alpha(x_1,x_2, \overset{(-)}{h}(x_1,x_2),t)\overset{(-)}{h}_{,\alpha} \\ & + \widetilde{v}_3(x_1,x_2,\overset{(+)}{h}(x_1,x_2),t) - \widetilde{v}_3(x_1,x_2,\overset{(-)}{h}(x_1,x_2),t).\end{aligned}$$

In the case under consideration i.e., when functions prescribed on the face surfaces are equal to zero (see notes before formula (48) and after formulas (48) and (49) below) (46) turns into the identity $0 = 0$.

Note that $2D$ approximate governing equations we have derived by direct integral averaging and then the obtained called the $N = 0$ approximation since it may be also obtained, from the Nth order approximation of hierarchical models constructed in [17] by I.Vekua's dimension reduction method [13], [14], [15] applied to fluids contained in prismatic shell-like domains, taking $N = 0$. I.Vekua himself used own method to elastic prismatic shells (see [13], [14]), where he also pointed out importance of investigation of BVPs for cusped prismatic shells (for survey of results in this direction see [21]).

5. The governing equations of subsections 4.1 and 4.2 for the case (3)

Let now $\mu = const$ and

$$\begin{aligned}& h(x_1,x_2) = h_0 x_2^\kappa, \quad \kappa = const \geq 0, \quad h_0 = const > 0, \quad 0 \leq x_2 \leq L \leq +\infty \\ & \omega := \{x_1, x_2 : 0 \leq x_2 \leq L \leq +\infty, \ -\infty \leq L_1 < x_1 < L_2 \leq +\infty\}.\end{aligned} \tag{47}$$

Then in the stationary case, neglecting volume forces, from (45) we have

$$x_2^2\Big(\overset{0}{w}_{30,11} + \overset{0}{w}_{30,22}\Big) + \kappa x_2 \overset{0}{w}_{30,2} - \kappa \overset{0}{w}_{30} = 0 \tag{48}$$

provided on the face surfaces velocities are zero and from (39), we have

$$x_2\Big(\overset{0}{\widetilde{v}}_{30,11} + \overset{0}{\widetilde{v}}_{30,22}\Big) + \kappa \overset{0}{\widetilde{v}}_{30,2} = 0 \tag{49}$$

provided on the face surfaces stress vectors are zero.

6. On Dirichlet and Keldysh type problems for an equation with type and order degeneration

Let us consider the equation

$$L(u) := y^m \frac{\partial^2 u}{\partial x^2} + y^n \frac{\partial^2 u}{\partial y^2} + a(x,y)\frac{\partial u}{\partial x} + b(x,y)\frac{\partial u}{\partial y} + c(x,y)u = 0, \tag{50}$$
$$m, n = \text{const} \geq 0,$$

in a domain ω (see Figure 22) bounded by a sufficiently smooth arc ω_1 lying in the upper half-plane $y \geq 0$ and by a segment $\overline{\omega}_0$ of the x-axis;

$$a, b, c, \in \mathcal{A}(\bar{\omega}),$$

$$c \leq 0 \text{ in } \bar{\omega}, \tag{51}$$

where $\mathcal{A}(\bar{\omega})$ is the class of functions analytic on $\bar{\omega}$ with respect to x, y.

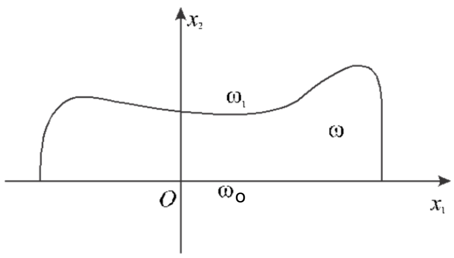

Figure 22. Projection of the $3D$ domain on plane $x_3 = 0$

Let us examine two boundary value problems:

Problem (Dirichlet Problem). Find $u \in C^2(\omega) \cap C(\bar{\omega})$ in ω from prescribed continuous values of $L(u)$ in ω and of u on the entire boundary $\partial\omega$.

Problem (Keldysh Problem). Find bounded $u \in C^2(\omega) \cap C(\omega \cup \omega_1)$ in ω from prescribed continuous values of $L(u)$ in ω and of u only on the part ω_1 of the boundary $\partial\omega$.

$C(\bar{\omega})$ is a set of functions continuous on closure of ω. $C^2(\omega)$ is a set of functions with continuous derivatives of orders ≤ 2 in ω.

Let

$$I_\delta := \{(x,y) \in \omega : \ 0 < y < \delta, \ \ \delta = \text{const} > 0\}. \tag{52}$$

Theorem 6.1 : *If*

either $n < 1$,

or $n \geq 1$ and

$$b(x, y) < y^{n-1} \ \text{ on } \ \bar{I}_\delta, \tag{53}$$

the Dirichlet problem is well-posed while the Keldysh problem has an infinite number of solutions.

If $n \geq 1$ and

$$b(x, y) \geq y^{n-1} \ \text{ in } \ I_\delta, \tag{54}$$

and in addition

$$a(x, y) = O(y^m), \quad y \to 0+ \tag{55}$$

(O is the Landau symbol), the Keldysh problem is well-posed while the Dirichlet problem, in general, has no solutions.

For the proof see [23] and compare with [24].

7. On well-posedness of BVPs for equations of Section 5

Clearly, when the effects of its viscosity may be supposed to be negligible, we get models for perfect fluids. Initial, contact, and boundary value conditions from classical ones we rewrite in the explained in the present paper way of passage to the moments. The governing equations are singular differential equations, in the case of angular $3D$ domains. On transparent examples it is shown that by investigating well-posedness of BVPs, boundary conditions may be nonclassical, in general.

In order to illustrate it we analyse two concrete examples when geometry of angular 3D domain is defined by

$$h(x_1, x_2) = h_0 x_2^\kappa, \ \ \kappa \geq 0, \ \ 0 \leq x_2 \leq L \leq \infty, \ \ L_1 < x_1 < L_2. \tag{56}$$

$L_1 = -\infty$, $L_2 = +\infty$ are admissible as well.

In this case we have to do with the two equations (48) and (49).

Equations (48) and (49) are singular PDEs, in other words PDEs with the order and type degeneracy with the order degeneracy line $x_2 = 0$.

Applying Theorem 6.1 we conclude:

For equation (48) $m = n = 2$ only (54), since $\kappa x_2 \geq x_2$ is fulfilled therefore. only the Keldysh Problem is well-posed and it's only then, when $\kappa \geq 1$.

For equation (49) $m = n = 1$ and since (53) for $\kappa < 1$ and (54) for $\kappa \geq 1$ are fulfilled and, therefore when $\kappa < 1$ the Dirichlet and when $\kappa \geq 1$ the Keldysh BVPs are well-posed.

We consider fluid flow in prismatic shell-like 3D domain when at the edge of the 3D domain tangent half-planes to the face surfaces create dihedral angle with line angle φ. It will be observed that considering viscous flow near the fixed dihedral angle, replacing the boundary condition $-$ velocity $v = 0$ on the edge by boundedness of velocity v in a neighborhood of the edge for $\kappa \geq 1$ i.e., $\varphi \in [0, \pi[$, in particular, of the mathematical cusp it means $\kappa > 1$, i.e., $\varphi = 0$, as it is in the case of the Keldysh problem. When the face surfaces smoothly pass each in other it means for

$\kappa < 1$ i.e., $\varphi = \pi$ the Dirichlet problem is well-posed and the boundary condition should be $v = 0$. These results are in a good accordance with the viscous boundary layer concept, according to experimental results of J. Nikuradse (see below Section 8).

A case of non-homogeneous viscosity is discussed as well.

7.1. *Case of a non-homogeneous fluid*

Let in addition

$$\mu(x_1, x_2) = \mu_0 x_2^{\kappa^*}, \ \ \mu_0, \kappa^* = const \geq 0, \ \ 0 \leq x_2 \leq L, \ \ L_1 < x_1 < L_2, \tag{57}$$

then from (45) we have

$$x_2^2 \overset{0}{\widetilde{v}}_{30,\alpha\alpha} + (\kappa + \kappa^*) x_2 \overset{0}{\widetilde{v}}_{30,\alpha} + \kappa(\kappa^* - 1) \overset{0}{\widetilde{v}}_{30} = 0.$$

Similarly to investigation of equation (48) for $(\kappa + \kappa^*) \geq 1$ (53) is fulfilled and hence only the Keldysh problem is well-posed under additional restriction $\kappa^* < 1$ [the last is needed in order to satisfy the condition (51). From (39) we get

$$x_2 \overset{0}{\widetilde{v}}_{30,\alpha\alpha} + (\kappa + \kappa^*) x_2^{\kappa+\kappa^*-1} \overset{0}{\widetilde{v}}_{30,\alpha} = 0, \tag{58}$$

$$(x_2^{\kappa+\kappa^*} \overset{0}{\widetilde{v}}_{30,\alpha})_{,\alpha} = 0, \tag{59}$$

i.e.,

$$x_2 \overset{0}{\widetilde{v}}_{30,\alpha\alpha} + (\kappa + \kappa^*) \overset{0}{\widetilde{v}}_{30,\alpha} = 0. \tag{60}$$

Similarly to investigation of equation (49), for $(\kappa + \kappa^*) < 1$ the Dirichlet problem is well-posed, while for $(\kappa + \kappa^*) \geq 1$ the Keldysh problem is well-posed (see p. 17).

8. About two experiments of Johhan (Ivane) Nikuradse. Conclusions of the present paper

While constructing and investigating hierarchical mathematical models for motion in angular containers of viscous fluid by Ilia Vekua's dimension reduction method it turned out that a usual (common) condition of sticking of the fluid at fixed wall was violated (inadmissible) which was mathematically expressed in that, that for well-posedness of BVP it was necessary instead of sticking of the fluid at dihedral edge to demand boundedness of the fluid velocity in a neighbourhood of the edge. In other words, in this case the Dirichlet boundary condition should be replaced by the Keldysh condition, i.e. the Dirichlet BVP is not well-posed in exchange for the Keldysh BVP which is well-posed. All that caused my interest to results of experiments in this field, e.g., to movement of fluids in pipes with angular cross-sections. From [11], [12] I found out two works of J. Nikuradse: [6] and [4].

[6] is devoted to experimental investigations of turbulent flows in non-circular pipes.

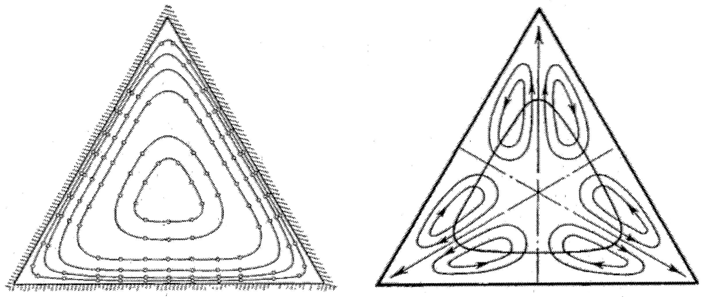

Figure 23.
a) equilaterally cross-section isotaches b) equilaterally cross-section secondary transversal stream

Here I quote the author (Nikuradse): "The task of the present work was to clarify the secondary movements in pipes with a non-circular cross-section on the basis of system tests. For this purpose, turbulent flows in such pipes were examined, namely, in pipes: 1) of triangular cross-section: a) equilateral, b) equilateral-rectangular and c) non-equilateral-rectangular; 2) of trapezoidal cross-section and 3) of circular cross-sections: a) with one groove and b) with two grooves. The work disintegrates into two parts: In the first part, the velocity distributions were measured and represented in the form of isotaches (i.e. lines of equal velocities of the main stream) which clearly show that the liquid flows into angles of the pipe cross-sections, divides into two parts there and returns. This causes whirls in the angles of the cross-sections. It has also been proven that the velocity grows along the bisectrix with the $\frac{5}{7}$th power of the distance from the angle tip. From the velocity distributions and the pressure slope, the shear stress distribution on the wall is calculated and illustrated graphically over the circumference of the pipe cross-section."

In other words, leading in a dye in the main stream J. Nikuradse experimentally established the existence of secondary transversal streams in angles of the cross-section that at firsts flows parallel to bisectrix and then with the decreased energy comes back along the isotach to core of the main stream which is out of the boundary layer. Thus, near the edge of dihedral angles will be formed whirls.

The form of the isotaches, i.e. of the lines denoting the same velocities of the main stream (see Fig. 23a) in the cross-section of the form of an equilateral triangle, is obtained when we have the Secondary transversal streams shown in Fig. 23b. L. Prandtl [25] theoretically justified the existence of these secondary transversal streams by constructing the so-called streamlines (a streamline is a line whose tangents at each point coincides with the direction of the velocity of a fluid particle at the same point, which means that at any moment of time the particle moves along the flow streamline).

Here from [4] I quote again the author (Nikuradse):
The report given here deals with the investigation of turbulent two-dimensional flows in canal-shaped expanded and narrowed canals (see Figure 21). The cross-section of the canal was a narrow rectangle, the narrow side was variable while the width remained constant. With this shape of the canals, one can expect that there will be a flat flow in the central part of each cross-section. The purpose of

the current work was to advance to greater divergence of the canals and to reach the area where the flow separates from the wall.

The velocity distribution was measured in two successive measuring transverse sections using a Pitot tube. The static pressure was determined at various points on the measuring plane by drilling into the wall. Since we were sufficiently far away from the inlet, the velocity profiles now change affinal, i.e. u/U is the same function of y/b in the two measuring cross-sections, where u is respective velocity, U means maximum velocity, y is distance from the middle of the canal, b is a half of the canal width (see Figure 21). Degrees below mean a half of opening angle, positive for divergent, negative for convergent canals. The divergence did not go beyond 4°, since with a larger expansion, around 5°, the flow already developed asymmetrical, i.e. rested against one wall, was pushed away from the other wall, and detachment from one wall occurred when the extension was only slightly elevated.

In [4] J. Nikuradse experimentally studied $2D$ turbulent flows in wedge shapely enlarged and narrowed canals, i.e. in divergent and convergent canals. In other words, the cross-section of the canal is a narrow rectangle. Moreover, a smaller side is variable, while that longer remarks constant. A half of the linear angle of the dihedral was -8, -4, -2, 0, 1, 3, 4, 6, 8. He found such an area when the flow detaches from the wall. Besides, in the zone of detaching constructed longitudinal velocity profile (it means he has measured velocities) (see also [11], [12]).

From the above it follows that our mathematical results of Section 7 show good agrement with experimental result of I. Nikuradse.

References

[1] G.B.L. Jeffery. *The two-dimensional steady motion of a viscous fluid*, The London, Edinburgh, and Dublin Philosophical Magazine and Journal of Science, **29**, 172 (1915), 455-465, https://doi.org/10.1080/14786440408635327

[2] G. Hamel. “Spiralförmige Bewegungen zäher Flüssigkeiten,” Jahresbericht der Deutschen Mathematiker-Vereinigung, **25** (1917), 34-60

[3] von Kármán, and Levi-Civita. “Vortrüge aus dem Gebiete der Hydro-und Aerodynamik,” 1922

[4] J. Nikuradse. *Turbulente Strömungen in keilförmigen Kanälen*, ZAMM, **8**, 424 (1928)

[5] J. Nikuradse. *Untersuchungen über die Strömungen des Wassers in konvergerten und divergenten Kanälen*, VDI-Forschungsheft, **289**, (1929)

[6] J. Nikuradse. *Untersuchungen über turbulente*, Strömungen in nichtkreisförmigen Rohren, Ing. Arch. B. I., (1930), S306

[7] W.R. Dean. *“LXXII. Note on the divergent flow of fluid,”* The London, Edinburgh, and Dublin Philosophical Magazine and Journal of Science, **18**, 121 (1934), 759-777

[8] L. Rosenhead. *“The steady two-dimensional radial flow of viscous fluid between two inclined plane walls*,” Proceedings of the Royal Society of London A: Mathematical, Physical and Engineering Sciences, **175**, 963 (1940), The Royal Society

[9] L. Landau, and E.M. Lifshitz, *“Fluid Mechanics Pergamon*,” New York **61** (1959)

[10] L.E. Fraenkel. *Laminar flow in symmetrical channels with slightly curved walls*, I. On the Jeffery-Hamel solutions for flow between plane walls, Proceedings of the Royal Society of London, Series A. Mathematical and Physical Sciences, **267**, 1328 (1962), 119-138

[11] R. Kavtaradze. J. *Nikuradse, Myth and Reality* (Georgian), Tbilisi, (2024), 156-158

[12] R. Kavtaradze. J. *Nikuradse, Myth and Reality* (Georgian), Tbilisi, (2023), 154-155

[13] I. Vekua. *On a way of calculating of prismatic shells* (Russian), Proceedings of A. Razmadze Institute of Mathematics of Georgian Academy of Sciences, **21** (1955), 191-259

[14] I. Vekua. *Shell Theory: General Methods of Construction*, Pitman Advanced Publishing Program, Boston-London, Melbourne, 1985

[15] G. Jaiani. *Cusped Shell-Like Structures*, Springer, Heidelberg-Dordrecht-London-New York, 2011

[16] G. Jaiani. *Theory of Cusped Euler-Bernoulli Beams and Kirchoff-Love Plates*, Lecture Notes of TICMI, **3** (2002), 132 p., Tbilisi University Press

[17] G. Jaiani. *Construction and investigation of differential hierarchical models for the Newtonian fluids*, Z Angew Math Mech., e202300251 (2024), https://doi.org/10.1002/zamm.202300251

[18] G. Jaiani. *Piezoelectric Viscoelastic Kelvin-Voigt Cusped Prismatic Shells*, Lecture Notes of TICMI, **19** (2018), 83 p., Tbilisi University Press

[19] S. Childress. *An Introduction to Theoretical Fluid Mechanics*, Courant lecture notes, 19, AMS, Providence, Rhode Island, 2009
[20] R. Dautray, J.-L. Lions. *Mathematical Analysis and Numerical Methods for Science and Technology.*, Vol. 1, Springer-Verlag, 1990
[21] G. Jaiani, N. Chinchaladze. *A survey of results on cusped standard and prismatic shells, in particular plates, and bars and on the corresponding singular PDEs, Continuum Mechanics and Thermodynamics*, **33** (2021), 1171-1198, Springer
[22] G. Jaiani. *Mathematical Models of Mechanics of Continua* (Second Edition) (Georgian), Tbilisi University Press, Tbilisi, 2018, 526 p.
[23] G. Jaiani. *On a generalization of the Keldysh theorem*, Georgian Mathematical Journal, **2**, 3 (1995), 71-84
[24] M.V. Keldysh. *On some cases of degeneration of an equation of eliptic type on the domain boundary* (Russian), Dokl. Akad. Nauk SSSR, **77**, 2 (1951), 181-183
[25] L. Prandtl. *Führer durch die Strömungslehre, 2*, Auflage, Göttingen, 1944